Physiologically based pharmacokinetic modeling of nanoparticles in rodents

By

XIAOWAN LI

A thesis submitted to the

Graduate School-New Brunswick

Rutgers, The State University of New Jersey

In partial fulfillment of the requirements

For the degree of

Master of Science

Graduate Program in Chemical and Biochemical Engineering

Written under the direction of

Charles M. Roth, PhD

And approved by

_____

_____

_____

_____

New Brunswick, New Jersey

January, 2017

ABSTRACT OF THE THESIS

Physiologically based pharmacokinetic modeling of nanoparticles in rodents

by XIAOWAN LI

Thesis Director:

Charles M. Roth, PhD

A variety of nanoparticles are under development for medicine, energy, food and cosmetics. Both organic and inorganic nanoparticles are playing an increased role in industrial and medical applications. However, little is known about their distribution and effects on the human body, and as a result concerns exist about potential health risks and safety problems. The long-term aim of this research is to quantify the distribution characteristics of nanoparticles and explore how the physicochemical properties of nanoparticles influence their distribution.

A physiologically based pharmacokinetic (PBPK) model was successfully developed to describe the pharmacokinetics and biodistribution of nanoparticles in various tissues and blood of the body. A PBPK model based on permeability-limited distribution from the vasculature to tissue spaces was compared with the PBPK model based on flow-limited distribution using literature values for distribution of nanoparticles. In general, the blood-flow limited model is not accurate enough to explain the complete biodistribution of nanoparticles, whereas the permeability-flow limited model provides a more faithful simulation. We also applied a novel formulation of the PBPK model, in which blood plasma kinetics are decoupled from tissue kinetics, and compared the description to those of traditional, coupled PBPK models. Our model parameterization suggested that the decoupled model method without elimination based on permeability-flow limited model accurately predicted

the trends of nanoparticles concentration in both tissue and blood. This could indicate that partition coefficients of tissues combining with blood flow to tissue might have a great influence on the biodistribution of nanoparticles.

This work provides a foundation for more accurate PBPK correlation of nanoparticle biodistribution that should be of utility both in the emerging area of nanotoxicology and in the preclinical drug development of nanomedicines.

ACKNOWLEDGEMENT

I would like to thank my thesis advisor Professor Roth of Department of Chemical and Biochemical Engineering at Rutgers, the State University of New Jersey, whose enthusiastic passion and discrete attitude towards computational chemistry and molecular simulations inspired me a lot. Dr. Roth consistently provided me research resources and give me valuable advice and help during my researches. He is always patient to help me with questions related to simulations processing and thesis writing and guided me in the right way towards the ultimate accomplishment.

I must express my truly deeply gratitude to my parents for providing me with sufficient support and continuous trust throughout my years of study and through my pursuit of Master degree in Chemical Engineering at Rutgers University. Thank you.

CONTENTS

List of Tables

List of Illustrations

CHAPTER 1 INTRODUCTION

1.1 Nanoparticles in the Body

The vastly increased production and use of nanoparticles in sectors including medicine, energy, food and cosmetics has increased the probability of exposure in the general environment.[1-2] Colloidal particles ranging in size between 10 nm and 1000 nm are well known as nanoparticles, which can be either inorganic or organic in chemical composition.[3] Due to the fact that nanoparticles are invisible and little is known about their toxicities, humans are concerned about potential health effects and safety problems.[4] The fate of nanoparticles within the human body is an active area of research that is growing with applications in the rapidly developing field of nanotechnology. On the other hand, in nanomedicine, nanoparticles encapsulating drugs or imaging agents are purposely introduced into the body for medical benefit. For nanoparticles of medical applications, their efficacy depends on the control of their distribution within the body, which also demands a clear illustration of the concentration-time profiles in organs and tissues of interest.[5]

Both organic and inorganic nanoparticles are of interest because of their uses in industrial and medical applications. Some examples of engineered inorganic nanoparticles include metal nanowires, metal oxides, and semiconductor quantum dots (QDs).[6] Quantum Dots (QDs) are a special class of fluorescent nanoparticles with superior optical properties when compared to organic dyes.[7-8] Although several different classes of QDs have emerged over the past couple of years, by far the most commonly used QDs are those prepared from semiconductor materials.[9] Although possessing the same crystal structure as the bulk semiconductor material, QDs consist of only a few hundred to a few thousand atoms. At certain sizes these nanoparticles behave differently from the bulk solid because of size quantization effects.[10]

Organic nanoparticles are of great interest in a variety of sectors. These include carbon nanotubes, fullerenes, as well as natural and synthetic polymers. Polymeric nanoparticles are playing an important role in the field of nanotechnology with a bunch of potential applications in clinical medicine, drug delivery, as well as some other researches. However, the scarcity of safe polymers with regulatory approval and their high cost have limited the wide spread application of nanoparticles to clinical medicine.[11] To overcome these disadvantages of polymeric nanoparticles, lipid nanoparticles have been introduced as an alternative carrier to offer the possibility to develop new therapeutics due to their special properties such as small size, large surface area, high drug loading and the interaction of phases at the interfaces, and are attractive for their potential to improve performance of pharmaceuticals and other materials.[12] Hence, lipid nanoparticles do have great perspectives for achieving the aim of controlled and site specific drug delivery and do have attracted plenty of prospective researchers.[13] So if lipid and polymeric nanoparticles are appropriately investigated, they may open new vistas in therapy and research.[14]

1.2 PBPK Model

The use of physiologically based pharmacokinetic (PBPK) models offers great potential to interpret existing data and guide predictions regarding the biodistribution and fate of nanoparticles. PBPK models have illustrated their potential usefulness for the study of the absorption, distribution, metabolism, and excretion (ADME) of small molecules and are beginning to be investigated for nanoparticles as well. PBPK models consist of multiple compartments corresponding to various tissues of the body, such as kidney, liver, muscle, skin, which are interconnected by the circulating blood system.[15] As such, they provide a framework for understanding the connections among the ADME processes. They have been used to quantify the distribution characteristics of drugs and drug carriers, and they are used clinically to estimate dose levels in preclinical models and in human clinical trials.[16] Furthermore, they can be used to adjust dosing based on mass or differences in metabolism.

In addition to the circulatory flow connections, the critical physiological component of a PBPK model is the description of how the drugs are distributed to the tissues. Each physiological compartment is divided into sub-compartments that correspond to vascular, tissue, and sometimes also cellular spaces, and the distribution among these can be generally described as being one of two types: permeability-limited tissue compartment models and flow-limited tissue compartment models.[17] Blood-flow limited kinetics tends to apply when the residence time of blood in each compartment is sufficiently long that equilibration occurs between the vascular and tissue sub-compartments. Generally, this condition is likely to be met by small lipophilic substances;[18] here, the blood flow to the tissue becomes the limiting process. Permeability-limited kinetics occurs for polar compounds and larger molecular structures that have difficulty penetrating the tissue; in this case, the permeability across the cell membrane becomes the limiting process. Consequently, the related PBPK models may exhibit different degrees of complexity. More specifically, determining blood flow rate should be fixed for flow-limited PBPK modeling but not for permeability-limited PBPK modeling. In our model, each tissue is considered to be a well-stirred compartment and assumed that elimination only happens in the kidney.

The general mass balance equation for each tissue compartment based on flow-limited tissue uptake is as follows,

$$\frac{dC_{tissue}}{dt} = \frac{Q_t}{V_t}\left(C_{blood} - \frac{C_{tissue}}{K_t}\right) \quad (1)$$

where V_t is the tissue volume, Q_t is the blood flow to tissue, $C_{arterial}$ equals C_{blood} is the arterial blood concentration, and K_t is the partition coefficient of nanoparticles between tissue and blood. Based on blood-flow limited model, all blood flows and tissue volumes which are fixed can be estimated from established physiological parameters, and the partition coefficients are estimated by fitting the model to

experimental data.

The general mass balance equation for each tissue based on permeability-limited tissue uptake is shown here,

$$\frac{dC_{tissue}}{dt} = \frac{P_t}{V_t}(C_{blood} - \frac{C_{tissue}}{K_t}) \quad (2)$$

where V_t is the tissue volume, P_t is the permeability of the tissue to solute transport, $C_{arterial}$ equals C_{blood} is the arterial blood concentration, K_t is the partition coefficient of nanoparticles between tissue and blood. While mathematically similar to the flow limited model, in the permeability-limited model, two physiological parameters -- the permeability (P_t) and partition coefficient (K_t) for each compartment are fit to data, while the tissue volume (V_t) remains constant using physiological data.

CHAPTER 2 MODEL DEVELOPMENT

2.1 Coupled Model Method

The coupled model consists of a set of *n* first-order ordinary differential equations, each of which corresponds to a material balance on one of the tissues or blood.[19] Here the dependent variable represents different concentrations of each important organ or tissue listed as an individual compartment, and the independent variable, *t*, is time starting from the point of nanoparticle administration. In one case study, our PBPK coupled model is composed of five different tissue compartments (skin, muscle, liver, kidney and a lumped tissue compartment for the rest of the body), as presented in Figure 1. However, the same structure can be generalized to different numbers of compartments depending on what is known about the biodistribution and on available data.

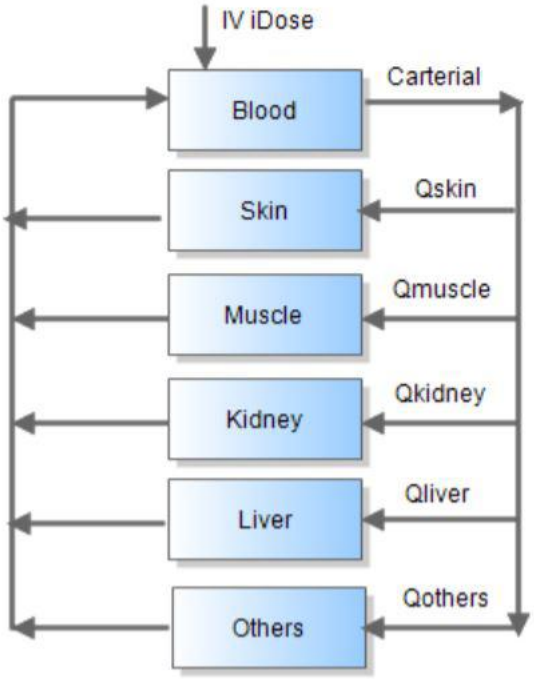

Figure 1. Constructed PBPK model describing the transportation of nanoparticles without elimination and metabolism occurred in any tissues.

The equations describing the rate of change of nanoparticle concentrations in each tissue are shown as follows for the blood flow-limited case.

$$\frac{dC_{Blood}}{dt}=\frac{(Q_{Skin}\times\frac{C_{Skin}}{P_{Skin}})+(Q_{Muscle}\times\frac{C_{Muscle}}{P_{Musle}})+(Q_{Kidney}\times\frac{C_{Kidney}}{P_{Kidney}})+(Q_{Liver}\times\frac{C_{Liver}}{P_{Liver}})+(Q_{Others}\times\frac{C_{Others}}{P_{Others}})-(C_{Blood}\times Q_{Tot})}{V_{Blood}} \tag{3}$$

$$\frac{dC_{Tissue}}{dt}=\frac{Q_{Tissue}\times[C_{Blood}-(\frac{C_{Tissue}}{P_{Tissue}})]}{V_{Tissue}} \tag{4}$$

In our PBPK model, no metabolism occurred in any tissues but we need to consider the possibility of the existence of elimination. Clearance (*CL*) can be defined as the volume of plasma which is completely cleared of drug per unit time. Clearance, which carries units of *L/h* , i.e. volume per time, can be defined for a tissue or for the whole body. Small molecule drugs are eliminated from the body primarily via the kidneys. Clearance is a useful term when talking of drug elimination since it characterizes the efficiency of the organs at elimination.

Incorporating clearance, the mass balance equation for kidney is changed as follows,

$$\frac{dC_{Kidney}}{dt}=\frac{Q_{Kidney}\times[C_{Blood}-(\frac{C_{Kidney}}{P_{Kidney}})]}{V_{Kidney}}-CL_k\cdot\frac{C_{Kidney}}{V_{Kidney}} \tag{5}$$

2.2 Decoupling Model Method

Fitting experimental data to muticompartment PBPK models requires solution of a multiparameter estimation problem in which the governing equations are ordinary differential equations that must be integrated in time. Furthermore, tissue distribution data tend to be sparse and noisy. On the other hand, accurate data can typically be obtained for drug/nanoparticle concentrations in the blood compartment. The Decoupled Model is a novel formalism that takes advantage of these facts by fitting the blood concentrations accurately and then using that fit to decouple the organ material balances.

The decoupling model involves first solving the equations describing the concentration of nanoparticle in the blood compartment. The decoupled equation for the blood compartment is then solved along with the original model equations (Coupled Direct Method), or separately (Decoupled Direct Method).[20] The decoupled method is advantageous both in terms of computational efficiency and stability of the solution. This method aims at transforming the complicated coupled equations into a system that can be solved sequentially.

2.2.1 Lumped two-compartment decoupling model with Elimination

We have assumed that the nanoparticle, once administered, is mixed instantaneously in the blood and subsequently distributes throughout the body, rapidly being taken up by the tissues or cleared from the body. We have in essence considered that the systemic circulation acts as a well mixed container. In that case, we can consider that the body is behaving as two distinct compartments: one for blood and the other a lumped representation of all other tissues.

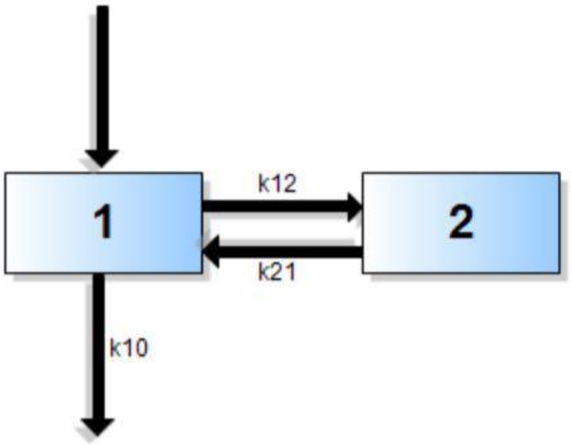

Figure 2. Schematic Diagram of the two compartment model with elimination

The differential equation for nanoparticle in the blood compartment following intravenous bolus administration is:

$$\frac{dC_{blood}}{dt} = -k_{10} \cdot C_{blood} - k_{12} \cdot C_{blood} + k_{21} \cdot C_{tissue} \tag{6}$$

The $k_{10} \cdot C_{blood}$ term describes elimination of the nanoparticle from the blood compartment, while the $k_{12} \cdot C_{blood}$ and $k_{21} \cdot C_{tissue}$ terms describe the distribution of nanoparticles between the blood and tissue compartments. Integration of this equation (using Laplace transforms) leads to a biexponential equation for plasma concentration as a function of time.

Thus,

$$C_{blood} = A \cdot e^{-\alpha \cdot t} + B \cdot e^{-\beta \cdot t} \tag{7}$$

The A, B, α, and β terms were derived from the micro-constants during the integration process where $A + B = \frac{DOSE}{V_0} = C_0$ and C_0 is the initial concentration.
So we can get,

$$C_{blood} = A \cdot e^{-\alpha \cdot t} + (C_0 - A) \cdot e^{-\beta \cdot t} \tag{8}$$

In that case, we can replace the concentration (Eq. 8) into which is in Eqs. 2.

$$\frac{dC_t}{dt} = \frac{Q_t}{V_t} \bullet [A \cdot e^{-\alpha \cdot t} + (C_0 - A) \cdot e^{-\beta \cdot t}] - \frac{Q_t}{V_t \cdot P_t} \bullet C_t \tag{9}$$

The solution of Eq. (9) is straightforward. By first integrating Eq. (9) yields a constant which could be solved by the initial condition which is zero. Then put the expression of this constant back to the equation. This is seen more clearly if the result is rewritten in the form using $\delta_t = \frac{Q_t}{V_t}$. The solution of equation 9 yields,

$$C_t = C_0 \cdot e^{-\frac{\delta_t \cdot t}{P_t}} + \delta_t \cdot P_t \left(\left(\frac{A}{\delta_t - \alpha \cdot P_t} \right) \left(e^{-\alpha \cdot t} - e^{-\frac{\delta_t \cdot t}{P_t}} \right) + \left(\frac{C_0 - A}{\delta_t - \beta \cdot P_t} \right) \left(e^{-\beta \cdot t} - e^{-\frac{\delta_t \cdot t}{P_t}} \right) \right) \tag{10}$$

2.2.2 Lumped two-compartment decoupled model without Elimination

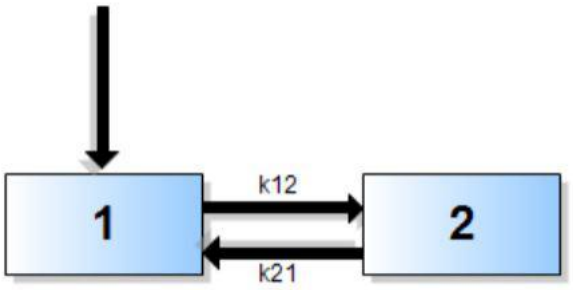

Figure 3. Schematic Diagram of the two compartment model without elimination

While pharmacokinetic models typically have a pathway for clearance of the drug, in the case of nanoparticles, clearance may frequently be slow or incomplete. As a result, we also investigated decoupled models without elimination of the nanoparticles. In this case, the differential equations describing nanoparticle concentration in the blood compartment and tissue compartment following intravenous bolus administration are given by:

$$V_{blood} \cdot \frac{dC_{blood}}{dt} = k_{21} \cdot V_{tissue} \cdot C_{tissue} - k_{12} \cdot V_{blood} \cdot C_{blood} \tag{11a}$$

$$V_{tissue} \cdot \frac{dC_{tissue}}{dt} = k_{12} \cdot V_{blood} \cdot C_{blood} - k_{21} \cdot V_{tissue} \cdot C_{tissue} \tag{11b}$$

The conditions at the boundaries are

$$C_{blood}(0) = C_0 \tag{12a}$$

$$C_{blood}(\infty) = C_{blood/ss} \tag{12b}$$

The steady state is an equilibrium between these two compartments. So we can conclude two equations as follows,

$$\frac{C_{blood/ss}}{C_{tissue/ss}} = \frac{k_{21}}{k_{12}} \tag{13a}$$

$$C_{blood/ss} + C_{tissue/ss} = C_0 \tag{13b}$$

Eqs. 11a and Eqs. 11b are coupled via $k_{21} \cdot V_{tissue} \cdot C_{tissue}$ term, which depends on the conditions at the boundaries. A second order differential equation is obtained by adding the equations. And after simplifying this second order differential equation, the result is

$$\frac{d^2 C_{blood}}{dt^2} + (k_{12} + k_{21}) \frac{dC_{blood}}{dt} = 0 \tag{14}$$

Integrating twice yields

$$C_{blood} = \int \delta \cdot e^{-(k_{12}+k_{21})t} dt \tag{15}$$

Where δ is a constant. Continuing solving C_{blood},

$$C_{blood} = -(\frac{\delta}{k_{12}+k_{21}}) \cdot e^{-(k_{12}+k_{21})\cdot t} + \gamma \tag{16}$$

Where γ and δ are constants. Then applying the two initial conditions (Eq. 12a) and (Eq.12b) into equation 16 yields,

$$\frac{C_{blood}}{C_o} = \left(\frac{k_{21}}{k_{12}+k_{21}}\right) + \left(\frac{k_{12}}{k_{12}+k_{21}}\right) \cdot e^{-(k_{12}+k_{21})\cdot t} \tag{17}$$

After defining $k_{12} + k_{21} = \partial$, equation 16 can be simplified as follows,

$$\frac{C_{blood}}{C_o} = 1 - \frac{k_{12}}{\partial}(1 - e^{-\partial \cdot t}) = 1 - k^*(1 - e^{-\partial \cdot t}) \tag{18}$$

Where $0 < k^* < 1$.

2.3 Model Solution

Matlab is a well-supported and mathematically oriented simulation software package that is clearly suitable for application to PBPK modeling.[21] Here Matlab (The MathWorks, Natick, MA), a powerful numerical computing tool, was used for physiologically based pharmacokinetic (PBPK) model implementation with respect to parameter estimation, including the estimation of partition coefficients and simulations of models. Values for physiologic parameters for mice and rats in the model were both obtained from literature,[6] in particular fraction of total cardiac output to different tissues and fraction of body weight to different tissues.

2.3.1 Coupled Model Solution

Code was separated into three files: the first file contained the rate equations and the parameters which we need to fit; the second contained a couple of code for special procedures that are frequently used (e.g., data obtained from both physiological parameters and experimental data from published studies[1], initial conditions for each tissues, code used to produce plots and estimate parameters, and so forth), while the third contained the procedure for minimizing the total sum of squares error with Jacobian matrix. In our case, the model file is typically identified by the *.m* file which holds experimental data and code procedure. Note that Matlab has the flexibility to place procedures in multiple *.m* files that may be readily called up while performing simulations.

In the second file, we should focus on numerical integration and parameter estimation. First, We used the routine ode45 in Matlab since it was recommended for most ODE problems and most of time, it will be your first choice of solver. But after testing ode45 which is a nonstiff solver, we found that ode45 is barely able to solve our model due to the extreme slow speed. The fact that this model exhibits stiffness is very clear. Both solvers gave similar results when incorporated within a parameter estimation scheme (Table 1). Table 1 summarizes the sum of squared errors for each

different tissues and total sum of squared errors based on blood-flow limited model using two different solvers, ode45 and ode15s.

Table 1. Sum of squared errors based on blood-flow limited model using two solvers.

SSE	Ode45	Ode15s
Blood	686.6671	688.3433
Skin	7.4286	7.3701
Muscle	3.2844	3.2195
Kidney	516.57	514.5304
Liver	126.8543	127.1705
Total	1340.8	1340.538

Under this circumstance, we chose to use ode15s which is a stiff solver.

For parameter estimation, partition coefficient in the flow-limited model or partition coefficient and blood flow in the permeability-limited model were both estimated by fitting the model to available experimental data. The standard Matlab version does not have a built-in likelihood function, so we used the constrained nonlinear optimization solver, *fmincon* within Matlab's Optimization Toolbox. *Fmincon* finds a constrained minimum of a scalar function of several variables starting at an initial estimate. This routine finds the parameter that minimizes the squared difference between the model predictions and the data.

In the third file, the Jacobian matrix can additionally be supplied to improve reliability and efficiency when using a stiff solver like ODE15s. The Jacobian matrix of the vector function *f* is the matrix of the derivatives of *f*. The example is presented as below.

$$J(x_1,...x_n)=\begin{bmatrix} \frac{\partial f_1}{\partial x_1} & \cdots & \frac{\partial f_1}{\partial x_n} \\ \vdots & \ddots & \vdots \\ \frac{\partial f_n}{\partial x_1} & \cdots & \frac{\partial f_n}{\partial x_n} \end{bmatrix} \tag{19}$$

Here f_n which is the dependent variable representing a set of differential equations in this PBPK model and x_n which is the independent variable representing the time period.

2.3.2 Decoupled Model Solution

One of biggest difference between decoupled model solution and coupled model solution is that for decoupled model, we need to solve the equation describing the concentration of nanoparticle in the blood compartment. The procedure is basically the same as the code of coupled model. The first file in the decoupled model merged the code of sum of squares error and the code of algebraic equation in the blood compartment together. The second file contained data, initial condition for blood compartment and *fmincon* optimization toolbox. Finally, we can find the best fitted equation for blood compartment. Then this equation can be applied to Equation 9 and the rest procedure would be very similar with coupled model solution.

CHAPTER 3 RESULTS AND DISCUSSIONS

The models were applied first to a case study based on the biodistribution of quantum dots (QDs) in mice. This data set was chosen because quantitative data were obtained in blood and four additional tissues over seven time points, making it relatively robust. In the following figures, the tissue concentration, C_t, is expressed as the percentage of the injected dose (ID) per g of tissue (% ID/g tissue). For QD705, the administered amount of cadmium which was 27.6 μg was used as ID.

The time course of QD705 in each compartment (Blood, Skin, Muscle, Kidney and Liver) is represented in Figure 4 and Figure 5. They respectively show the comparisons between the results from PBPK model simulations based on different methods and the experimental data on tissue and blood concentrations of QD705. Specifically, simulations from the model based on blood-flow limited distribution were compared with data in Figure 4 and simulations based on permeability-limited distribution were compared in Figure 5.

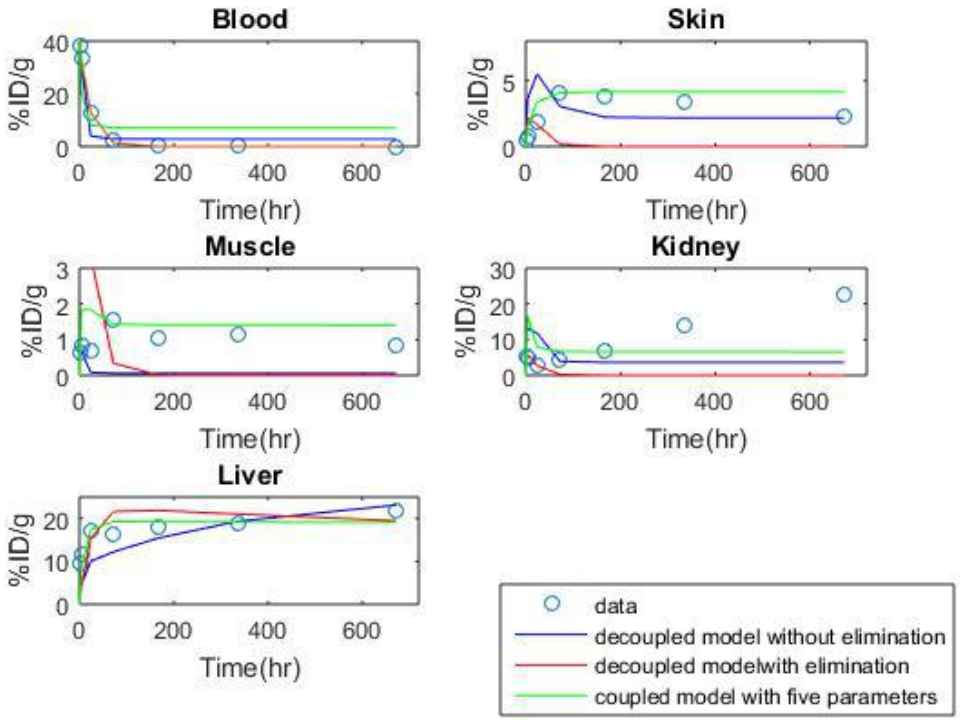

Figure 4. Comparisons of decoupled model(blood-flow limited) both with and without eliminations and coupled model. Each symbol represents the experimental data from Literature. The blue solid line represents the decoupled model without elimination; the red solid line represents the decoupled model with elimination and the green line represents coupled model without elimination based on optimized tissue-to-blood partition coefficients.

The blood profile in Figures 4 depicts blood concentration-time profiles for QD705 after i.v. administration. It appears from the graphs that the model captured the blood concentration time profiles relatively well for these three different models, though the models without elimination showed long-term retention of nanoparticles in the blood to a greater extent than observed experimentally. And these models predicted an increase to steady-state concentration within a very short time. Since the blood-flow limited model did not contain metabolism of nanoparticles, it showed persistent concentrations in the tissues for 28 days. Concentration versus time profiles for Skin, liver, kidneys and muscle were captured by the PBPK model as depicted in Figure 4. Concentration-time curves of these organs went up first within a short time and came down until reaching steady-state in all the tissues. Among these well-stirred

organs, QD705 distributed most extensively into kidneys and liver. The extent of distribution into skin and muscle was moderate.

The decoupled model with elimination forces all material to leave the body, thus it predicts all concentrations go to zero at long times, though in the case of liver a slow decay rate is fit. In the experimental data, while the blood concentration does go to zero, the nanoparticles are retained in the tissues over the full duration where data are available (0 to 28 days). The reason for the extra accumulation of QDs in the kidney at later time was still unclear. As a result, the models generally do a poor job of fitting data that are increasing with time, as is observed here in the kidney. The increasing in the kidney concentration might be due to the redistribution from other body tissues like spleen and skin to the kidney, where they may become relatively "stuck".

The sum of squared errors of prediction (SSE), is the sum of the squares of residuals (deviations predicted from actual values of data). It is a measure of the difference between the data and an estimation model. A small sum of squared errors indicates a better fit of the model to the data. It is used as an optimality criterion in parameter and model selection.

Table 2 summarizes the sum of squared errors for each method, based on blood-flow limited model. By decoupling the tissue compartments from the blood, a more accurate fit is obtained as measured by the total sum of squared errors. This is because we can minimize the sum of squared errors from blood fit first by decoupling the tissue compartments. The decoupled model method did a better job on fitting blood data than the coupled model method. Although the decoupled model without elimination does not fit the blood data as well as that with elimination, it provides a fit with less error in the other tissue compartments.

Table 2. Sum of squared errors for each method, based on blood-flow limited model.

SSE	Decoupled Model		Coupled Model
	With elimination	Without elimination	
Blood	1.9089	205.408	688.3433
Skin	48.2105	27.1432	7.3701
Muscle	104.1972	5.5233	3.2195
Kidney	782.3521	632.7734	514.5304
Liver	197.4452	196.2048	127.1705
Total	1134.1139	1067.0546	1340.538

All of the flow-limited models overestimate the initial rate of distribution from blood to tissues, as they assume rapid equilibration between blood and tissue. The initial tissue uptake is driven by the ratio Q_t/V_t and is thus fixed by these physiological parameters. In a permeability-limited model, as the name suggests, the distribution of the nanoparticle is dictated by a rate-limiting entry step. The values of nanoparticle permeability for various tissues are not known and instead must be fit, doubling the number of fit parameters, from *n* to *2n* in the coupled models and from 1 to 2 per tissue in the decoupled models. Because the permeability is a fit parameter, the initial uptake kinetics can be fit more accurately.

The predictions from the PBPK model with estimated partition coefficients and estimated permeability for various tissues are plotted against the measured data from the studies as shown in Figure 5.

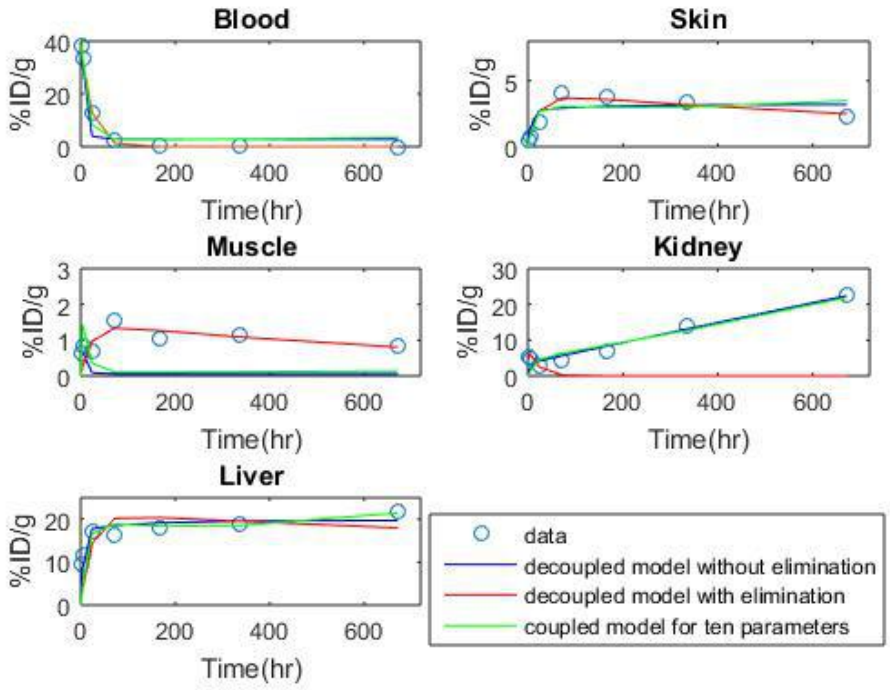

Figure 5. Comparisons of decoupled model(permeability limited) both with and without eliminations and coupled model. Each symbol represents the experimental data from Literature. The blue solid line represents the decoupled model without elimination; the red solid line represents the decoupled model with elimination and the green line represents coupled model without elimination based on optimized tissue-to-blood partition coefficients and optimized permeability for various tissues.

Comparing between Figure 4 and Figure 5, the red line which represents the decoupled model with elimination shows all concentrations go to zero, which is similar in both figures. One of the biggest difference between Figure 4 and Figure 5 is in the simulations of kidney concentration. In Figure 4, it is very obvious that even though the kidney data is going up in the later time points, the simulation based on blood-flow limited model remains straight over time. But in Figure 5, both simulations from decoupled model method without elimination and coupled model method based on permeability-limited shows are consistent with the kidney data. Thus, through the use of two parameters in kidney, the permeability-limited model's predictions fit the experiment measurements relatively well compared to blood-flow limited model's predictions.

Table 3 summarizes the sum of squared errors in each different methods based on permeability-flow limited model. Compared to the values in table 2, we can conclude that the permeability- flow limited model provides a better fit (less total error) than the blood-flow limited model. Among them all, we can get a conclusion that the decoupled model without elimination did the best job in all these six different methods. This is likely due to a combination of more accurately reflecting the physiology of the nanoparticle uptake process as well as the fitting of additional parameters.

Table 3. Sum of squared errors for each method based on permeability-limited model.

SSE	**Decoupled Model**		**Coupled Model**
	With elimination	**Without elimination**	
Blood	1.9089	205.408	454.4576
Skin	0.9875	3.8207	5.2636
Muscle	0.8603	5.5164	7.0047
Kidney	777.6848	39.2847	52.8044
Liver	189.92	74.4519	112.4464
Total	971.3616	328.4816	631.7016

The potential mechanisms for the biodistribution of nanoparticles are very complicated. Several factors such as interactions with nanoparticles properties and biological barriers (size, composition, size and surface modifications) have been shown to significantly affect the biodistribution of nanoparticles.[22] Our study indicated that partition coefficients of tissues combining with blood flow to tissue might have a great influence on the biodistribution of nanoparticles. Furthermore, nanoparticles are reportedly readily uptaken by phagocytic cells in the liver, spleen, lung, and kidneys.[23] Proteins associated with the surfaces of nanoparticles are recognized by macrophages and might modulate the translocation and redistribution of nanoparticles from blood by organs with an reticuloendothelial system.[24]

CHAPTER 4 CONCLUSION

The development of a PBPK model reflects the current limitations of our understanding of important biological processes that help identify data gaps. Simulation of the experimental data could somehow fill gaps in experimental data. Also the PBPK model could aid in finding factors that influence the nanoparticle distribution and further improving efficacy and reducing toxicity of nanoparticles. This study estimated and identified important parameters affecting the performance of PBPK models in various organs and tissues despite certain data limitations. By considering both flow-limited model and permeability-limited models from different methods, we increased the predictability of the PBPK model for actual data. The general patterns of biodistribution of nanoparticles in mice were captured accurately in the model simulations. The final aim of most nanoparticle studies are their application in humans. The PBPK model allows us to understand and mimic drug kinetics in organs and tissues that are not accessible in humans and provide the possibility of applying models to humans, which will greatly enhance applications of nanoparticles.[25]

The PBPK model worked quite well to nanoparticles for simulating biodistribution. In general, the blood-flow limited model is not appropriate enough to explain the completed pharmacokinetics, but the permeability-flow limited model is more capable to describe than the blood-flow limited model from the model simulation. More importantly, the decoupled model without elimination based on permeability flow-limited model accurately predicted the trends of nanoparticles concentration in both tissue and blood in mice. This could indicate that partition coefficients of tissues combining with blood flow to tissue might affect the biodistribution of nanoparticles. Since we have shown in this analysis that due to the good description of nanoparticle in mice, we may have faith to simulate nanoparticle concentration-time profiles in tissues of interest in humans.

In this study, we established a potentially predictive dynamic model for nanoparticles, which we have to investigate more comprehensively in future studies. This work provides a foundation for more accurate PBPK correlation of nanoparticle biodistribution and contributes to a better understanding of the fundamental processes. But additional studies on different factors, such as size of nanoparticles, are needed to better understand and to characterize the time course for biodistribution of nanoparticles. PBPK models might can be coupled with pharmacodynamics[26] and toxicity models.[27] The PBPK model of nanoparticles and nanoparticle drug carrier delivery kinetics can be combined together. Such a model will be capable to describe the effects of nanoparticle distribution and drug release kinetics on the pharmacokinetics of drugs.

REFERENCES

1. Kostarelos, K. (2006). "The emergence of nanomedicine: a field in the making." Nanomedicine **1**: 1–3.

2. Dobrovolskaia, M. A., et al. (2007)." Immunological Properties of Engineered Nanomaterials." Nat. Nanotechnol **2**: 469–478.

3. Mukherjee, S., et al. (2009). "Solid lipid nanoparticles: a modern formulation approach in drug delivery system." Indian journal of pharmaceutical sciences **71**(4): 349.

4. Wenger, Y., et al. (2011). "Tissue distribution and pharmacokinetics of stable polyacrylamide nanoparticles following intravenous injection in the rat." Toxicology and applied pharmacology **251**(3): 181-190.

5. Michalet, X., et al. (2001). "Properties of fluorescent semiconductor nanocrystals and their application to biological labeling." Single Molecules **2**(4): 261-276.

6. Yang, R. S., et al. (2007). "Persistent tissue kinetics and redistribution of nanoparticles, quantum dot 705, in mice: ICP-MS quantitative assessment." Environmental Health Perspectives: 1339-1343.

7. Medintz, I. L., et al. (2005). "Quantum dot bioconjugates for imaging, labelling and sensing." Nature materials **4**(6): 435-446.

8. Andersen, K., et al. (2002). "Quantum confinement in CdSe nanocrystallites." Journal of Non-Crystalline Solids **299**: 1105-1110.

9. Tomasulo, M., et al. (2006). "pH-sensitive quantum dots." The Journal of Physical Chemistry B **110**(9): 3853-3855.

10. El-Eskandarany, M. S., et al. (1997). "Cyclic crystalline-amorphous transformations of mechanically alloyed Co75Ti25." Applied physics letters **70**(13): 1679-1681.

11. Üner, M. (2006). "Preparation, characterization and physico-chemical properties of solid lipid nanoparticles (SLN) and nanostructured lipid carriers (NLC): their benefits as colloidal drug carrier systems." Die Pharmazie-An International Journal of Pharmaceutical Sciences **61**(5): 375-386.

12. Scheffel, U., et al. (1972). "Albumin microspheres for study of the reticuloendothelial system." Journal of Nuclear Medicine **13**(7): 498-503.

13. Uner M. Preparation, characterization and physico-chemical properties of solid lipid nanoparticles (SLN) and nanostructured lipid carriers (NLC): Their benefits as colloidal drug carrier systems. Pharmazie 2006;61:375-86.

14. Gasco, M. R. (1993). Method for producing solid lipid microspheres having a narrow size distribution, Google Patents.

15. Li, M., et al. (2010). "Physiologically based pharmacokinetic modeling of nanoparticles." ACS nano **4**(11): 6303-6317.

16. Reddy, M., et al. (2005). Physiologically based pharmacokinetic modeling: science and applications, John Wiley & Sons.

17. Jones, H. M., et al. (2009). "Modelling and PBPK simulation in drug discovery." The AAPS journal **11**(1): 155-166.

18. Bois, F. Y., et al. (2010). "PBPK modelling of inter-individual variability in the pharmacokinetics of environmental chemicals." Toxicology **278**(3): 256-267.

19. Lee, H. A., et al. (2009). "Comparison of quantum dot biodistribution with a blood-flow-limited physiologically based pharmacokinetic model." Nano letters **9**(2): 794-799.

20. Isukapalli, S. S. (1999). Uncertainty analysis of transport-transformation models, Citeseer.

21. Easterling, M. R., et al. (2000). "Comparative analysis of software for physiologically based pharmacokinetic modeling: simulation, optimization, and sensitivity analysis." Toxicology Methods **10**(3): 203-229.

22. Weijs L, Yang RS, Covaci A, Das K, Blust R. Physiologically based pharmacokinetic (PBPK) models for lifetime exposure to PCB 153 in male and female harbor porpoises (Phocoena phocoena): model development and evaluation. Environ Sci Technol. 2010;**44**:7023–7030.

23. Moghimi SM, Hunter AC, Murray JC. Long-circulating and target-specific nanoparticles: theory to practice. Pharmacol Rev. 2001; **53**:283–318.

24. Li SD, Huang L. Nanoparticles evading the reticuloendothelial system: role of the supported bilayer. Biochim Biophys Acta. 2009;**1788**: 2259–2266.

25. Stern, S. T., et al. (2010). "Translational considerations for cancer nanomedicine." Journal of Controlled Release **146**(2): 164-174.

26. Timchalk, C., et al. (2002). "A physiologically based pharmacokinetic and pharmacodynamic (PBPK/PD) model for the organophosphate insecticide chlorpyrifos in rats and humans." Toxicological Sciences **66**(1): 34-53.

27. Liao, C.-M., et al. (2005). "Dynamical coupling of PBPK/PD and AUC-based toxicity models for arsenic in tilapia Oreochromis mossambicus from blackfoot disease area in Taiwan." Environmental pollution **135**(2): 221-233.

Appendix

Table 4. Physiological parameters used to calculate the values of Q_t and V_t:

MOUSE	Skin	Muscle	Kidney	Liver	Other	Blood
fQC	0.09	0.28	0.15	0.16	0.32	
Q_t(L/h)	0.099238	0.308739	0.165396	0.176422	0.352845	1.10264
fV	0.17	0.38	0.017	0.055	0.37	0.049
V_t(g)	6.086	13.604	0.6086	1.969	13.246	1.7542

RAT	Skin	Muscle	Kidney	Liver	Other	Blood
fQC	0.058	0.28	0.14	0.17	0.35	
Q_t(L/h)	0.288544	1.392972	0.696486	0.845733	1.741215	4.9749
fV	0.19	0.4	0.007	0.03	0.26	0.074
V_t(g)	58.71	123.6	2.163	9.27	80.34	22.866